# Chapter 7 – Materials and Methods

The preceding pages address some of the factors that should be considered when designing a methodology for the measurement of bone density. The methodology presented here can be conveniently split into two parts: material selection and method design. This section will describe in full the experimental material that will be used in this project. It will then present the methodology that will be employed to obtain density data from the material. Finally, the methodology will be tested, to ensure that the data produced are reliable. It will draw on the previous chapter, to ensure that the material and methods used here are suitable to address the requirements of this project.

## 7.1: Materials

### 7.1.1: Taxon choice

Section 6.4.2 summarises the description of previously employed methodologies by noting that in every case, previous researchers have targeted the taxon most able to fulfil their specific research criteria. This project will address the density of modern sheep bones. Sheep is the most common taxon recovered from the majority of Neolithic and post-Neolithic European and Asian archaeological sites. This is certainly the case for the animal remains recovered so far from Çatalhöyük (the site to which the bone density data produced by this project will later be applied - see chapter 9), where they almost certainly formed a major part of the daily diet. Given these facts, it seems that the natural choice of taxon for analysis in this project is sheep. The choice of sheep as the taxon of study for this project ensures that the results produced will be especially suitable for the analysis of the animal remains from Çatalhöyük. They will also have a broad applicability to a significant number of sites over a large geographical area.

By selecting sheep as the only taxon to be studied, it will be possible to maximise the sample size and so the data produced will be less prone to distortion by atypical individuals (see section 6.4.1). A further advantage of selecting sheep as the target taxon is that the data produced can be contrasted or combined with those produced by Binford and Bertram (1977), Brain (1969) and Lyman (1984).

### 7.1.2: Element selection

Section 6.4.3 described the criteria that should be used when selecting elements for density measurement. These include consideration of economic factors and butchery, identification and ageing potential and the compatibility of the recovered data with the archaeological recording systems concerned. According to these criteria, and those laid down by Lyman (1984 p273) (see section 6.2.5), the following elements have been selected for analysis: scapula, humerus, radius, metacarpal, pelvis, femur, tibia, metatarsal and first phalanx. The astragalus, third phalanx, skull, carpals and tarsals have been omitted, because, since they do not fuse, they cannot provide the same level of age information as the other bones. The calcaneus, ulna and second and third phalanges often act as "riders" (Binford 1978) when looking at carcass utilisation and butchery patterns, therefore the body part information provided by these bones is the same as that provided by the associated long bones. The vertebrae and ribs will not be measured, because many zooarchaeological recording systems, including that used at Çatalhöyük, do not identify these elements to taxon, but instead place them in a size category. Consequently, data on the density of vertebrae and ribs of sheep will be of limited use, since they will only be able to be applied to "sheep sized" archaeological material which might include, for example, dogs or young pigs. Finally, mandibles are omitted from this study because, although they provide good aging data for archaeological animals, these are not consistent with those provided by fusion patterns. Fusion is to be the means by which age is determined for the archaeological material in this project, because it applies to a great many more elements than dental methods. Since they do not provide fusion data, density data from mandibles would be of limited value.

Once density values for all of the experimental material had been established, it emerged that the inclusion of density values for mandibles would have markedly increased the interpretative power of this project. On reflection, the value of data relating to mandible densities would have outweighed the methodological problems involved in their production.

By omitting these elements and analyzing density data from scapula, humerus, radius, metacarpal, pelvis, femur, tibia, metatarsal and first phalanx only, it will be possible to examine a much larger number of individuals.

### 7.1.3: Scan-site selection

The summary of previously employed methodologies in section 6.4.4 noted that points on a bone where density measurements are to be taken should be chosen according to the four criteria proposed by Lyman (1984 p273). Also, the selected sites must be compatible with the Çatalhöyük recording system and must be in such a position that they can be reliably and repeatedly located.

A valuable aspect of the faunal recording system at Çatalhöyük is that for each bone fragment recovered the presence or absence of any "diagnostic zones" is recorded. Diagnostic zones (DZs) are parts of bones that were first defined by Watson (1972) and are intended to represent parts of bones that are easily identified and are commonly recovered. DZs are also often the same regions of the skeleton that provide fusion (and therefore age) data. If more than 50% of any one DZ is recorded as being present in an archaeological bone fragment, then that portion of the bone (usually proximal or distal end) is recorded as present. In practice, DZs are usually the fusion planes of a bone's diaphysis. Diagnostic zones are to form the basis of the selection of scan-sites for this study. This will mean that the density values refer to the precise parts of each bone which are specifically recorded as being either present or absent at Çatalhöyük. Occasionally it will be necessary to locate scan-sites to specific parts of a bone for other reasons, such as in the case of the metapodia. In this case, scan-sites will be positioned away from the center of the DZ, since in the central area of the metapodia of artiodactyls is a fusion plane between the very early fusing third and fourth metapodia. Consequently, the central area may not prove to be a reliable scan-site. In addition, placing the scan-site to one side, over the third metapodia, has the advantage that measurements from very young individuals (whose metapodia have not yet fused) and other taxa (eg horse, whose metapodia do not fuse) can be more reliably compared.

In addition, the density of the shaft of the long bones and metapodia will be measured. In these cases, the scan-sites will be located at the mid-point of each bone shaft. Taking the measurement at the mid-point has the advantage that the same point can be repeatedly identified on different occasions or on different bones without reference to bone "landmarks" of which bone shafts have comparatively few. The position of each scan-site is shown in figure 7.1. A more detailed description of each scan-site can be found in appendix A.

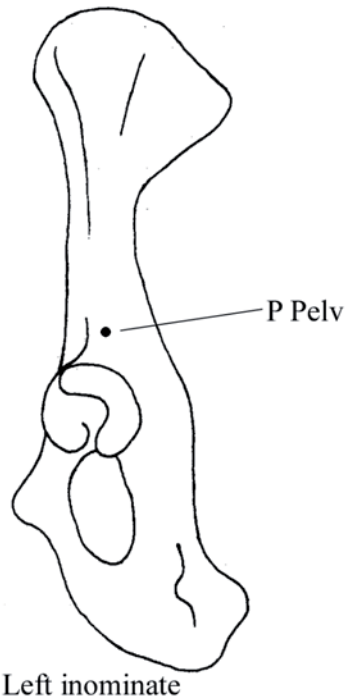


Left inominate
lateral view

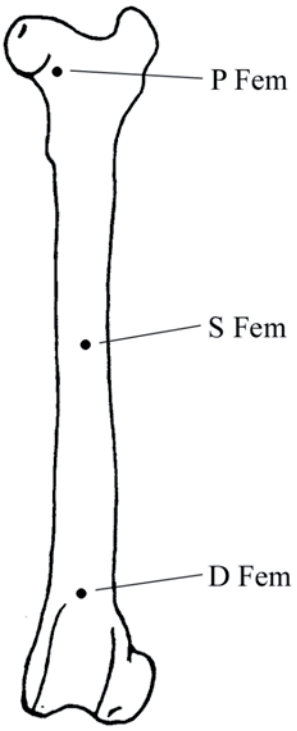


Left femur
anterior view

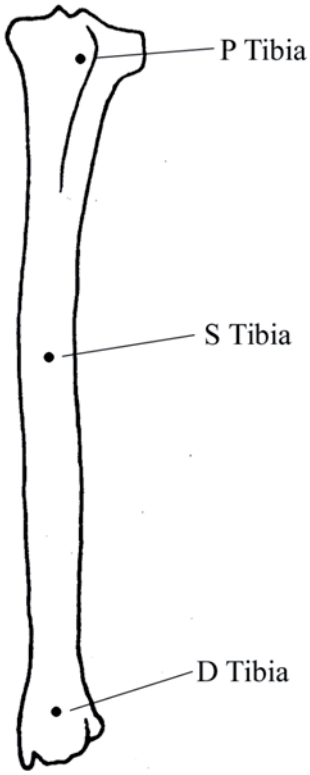


Left tibia
anterior view

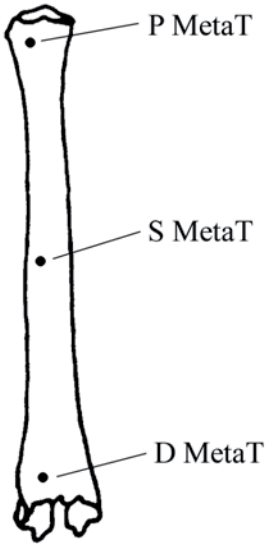


Left metatarsal
anterior view

*Continued* ⟶

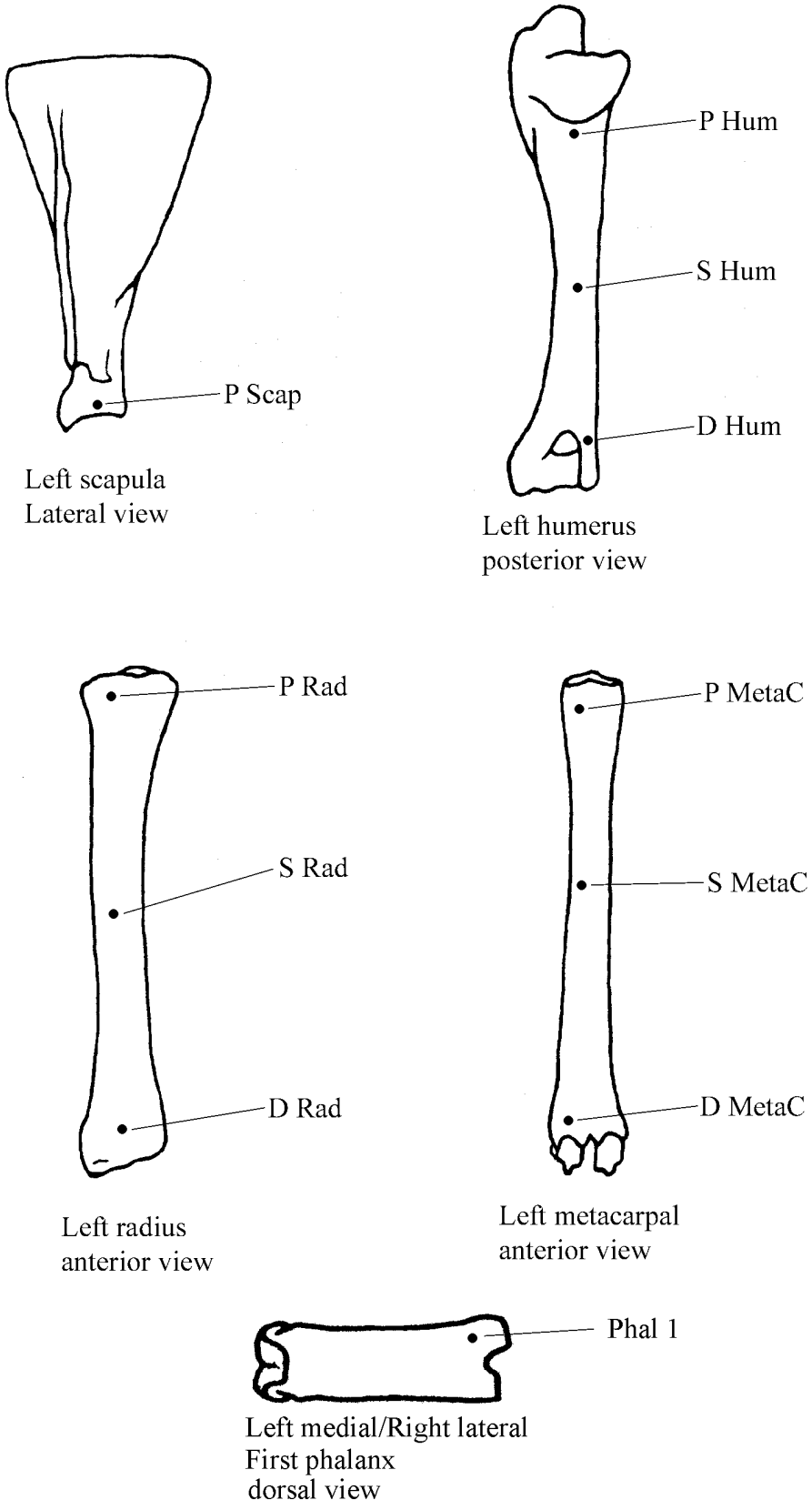


***Figure 7.1: Showing the location of each of the scan-sites to be used in this project. The illustration is based on that presented by Lyman (1984 pp274 - 275, Fig 2 (Section 6.2.5, figure 6.1 in this thesis) to facilitate comparison between the two. The names given to the scan-sites are explained below.***

The scan-sites defined in this project have the advantage that they overlap with some of the scan-sites selected by Lyman (1984 pp274 - 275) (see section 6.2.5). This means that the data produced by this project can be compared or combined with those produced by Lyman (1984) and other researchers who based their scan-sites on Lyman's (eg Kreutzer (1992), Elkin (1995) and Lam *et al* (1999)). The scan-sites chosen for this project (including their abbreviations – as used here) and the equivalent scan-sites defined by Lyman (1984 p274 - 275) are given below.

| **Scan-site used in this project** | **Scan-site used by Lyman** |
|---|---|
| Scapula (*Scap*) | SP1 |
| Proximal Humerus (*P Hum*) | HU2 |
| Humerus Shaft (*S Hum*) | HU3 |
| Distal Humerus (*D Hum*) | HU5 |
| Proximal Radius (*P Rad*) | RA2 |
| Radius Shaft (*S Rad*) | RA3 |
| Distal Radius (*D Rad*) | RA4 |
| Proximal Metacarpal (*P MetaC*) | MC2 |
| Metacarpal Shaft (*S MetaC*) | MC3 |
| Distal Metacarpal (*D MetaC*) | MC5 |
| Pelvis (*Pelv*) | IL2 |
| Proximal Femur (*P Fem*) | FE1 |
| Femur Shaft (*S Fem*) | FE4 |
| Distal Femur (*D Fem*) | FE5 |
| Proximal Tibia (*P Tib*) | TI1 |
| Tibia Shaft (*S Tib*) | TI3 |
| Distal Tibia (*D Tib*) | TI5 |
| Proximal Metatarsal (*P MetaT*) | MR2 |
| Metatarsal Shaft (*S MetaT*) | MR3 |
| Distal Metatarsal (*D MetaT*) | MR5 |
| First Phalanx (*Phal1*) | P11 |

Now that the taxon, elements and scan-sites used in this project have been described and justified, it is possible to describe the source and attributes of the material that was measured.

### 7.1.4: Material source

Section 6.4.5 explains why it is necessary for this project to use animals from a modern reference collection, with known life histories, as the material to be measured. In the case of this project, sheep skeletons from English Heritage's Ancient Monuments Laboratory (AML) were used. The AML is based in Fort Cumberland, Portsmouth, and

holds a large number of modern skeletons (partial and complete) of a wide variety of taxa (see Corke *et al* (1997) for a full list). The AML collection is intended primarily as a comparative collection. It consists of a combination of animals purchased for specific research purposes and those that were donated to the collection. The material was borrowed from AML with the kind permission of Dr Simon Davis and Dr Poly Baker.

The AML material used here was gathered from a wide range of sources across Britain between 1964 and 1999. The animals had therefore lived under a variety of environmental and management conditions. It is worth noting that animals number 15, 48, 65, 70, 71, 73, 74, 78 and 80 were from the same flock (from Newmarket, Suffolk). When the skeletons from this flock were prepared, it was noted that they were all suffering from osteoporotic lesions on their mandibles (pers comm E. Corke). Whether these lesions were due to environmental or genetic factors is not certain, but it is possible that the cause of these lesions will manifest itself in other parts of the skeleton.

## 7.2: Material Attributes

The material from the AML was particularly well suited to a project of this type because a relatively large amount of information regarding each skeleton was available. Details of each individual's age, sex, date of birth, date of death, breed, farm of origin and preparation method (the method employed to deflesh and clean the animals) were usually available. Some individuals had details of their weight or condition at death and mode of death. All such information was recorded on a database specifically designed for this project. This database can be viewed in its entirety in appendix B. Since the animals were not raised specifically to act as experimental material for this project, the information regarding them was occasionally lacking. It will become apparent in the next chapter that more information might have aided interpretation of the results produced by this project. However, the information available was quite sufficient to carry out the analyses described below.

A total of 95 individuals were examined ranging from between 0 days (stillbirths) and 4791 days in age. This was the total number of available individuals of known age at death. In order to characterize the material in terms of these variables it would be advantageous to specify the variables that are of importance to this project. These are the ones that are suspected to have an impact on the density of an animal's bones. These are breed, sex, preparation method, month of death and age. The potential for these factors to affect the density of a skeleton has already been discussed (see section 5.2). Other factors that might affect bone density (such as nutritional status and

disease) cannot be described or examined in this project because little or no information regarding these variables was available.

### 7.2.1: Breed

The material came from a wide variety of breeds. There were 25 Soays and 52 Shetlands. The 18 other individuals consisted of Clun Forest, Hebridean, Herdwick, Manx Loughtan, Moorit, North Ronaldsay, Texel-Mule cross and Suffolk-Blackface cross. The distribution of the sample for each of the breeds is graphically displayed in table 7.1.

| Breed | Soay | Shetland | Clun Forest | Hebridean | Herdwick | Manx Loughtan | Moorit | North Ronaldsay | Texel X Mule | Suffolk X Blackface |
|---|---|---|---|---|---|---|---|---|---|---|
| Number of individuals analyzed | 25 | 52 | 4 | 1 | 3 | 5 | 1 | 1 | 1 | 2 |

***Table 7.1: Showing the number of animals in the experimental material from each breed.***

It is clear that breeds other than Soays and Shetlands were poorly represented in the experimental material. It was therefore decided to group them as a single category, labeled “other”, since by themselves each of these breeds does not have a large enough sample to serve as an analytical category. Very few animals had information relating to their parental or other close genetic associations. In fact such information was only available for animals number 1019, 1020 and 1021 (the former being the mother of the latter two, stillborn, animals). Consequently, although the breed of an animal and the flock from which it came can be established, the precise ways in which different animals were related cannot be determined.

### 7.2.2: Sex

The sex of each animal was recorded as male, female or castrate. The 95 animals measured consisted of 17 males, 41 females and 37 castrates. Since insufficient information on the matter was available, castrates were assumed to have been castrated in the first few weeks of life.

### 7.2.3: Preparation method

Elaine Corke undertook the task of defleshing the majority of the material. The recording of the preparation method used to deflesh each animal was occasionally lacking (especially in the case of the material collected a considerable time ago). However, given the potential impact of preparation techniques on the density of the material, a system of categories was devised to characterize the processes to which the material had been subjected. These were: boiling, simmering, maceration, burial and "unknown". The numbers of animals prepared by each of these methods is shown in table 7.2.

| Preparation Method | Boiling | Simmering | Maceration | Burial | Unknown |
|---|---|---|---|---|---|
| Number of individuals analyzed | 11 | 9 | 24 | 20 | 31 |

***Table 7.2: Showing the number of animals in the experimental material defleshed by each of the preparation methods.***

Of the 11 individuals prepared by boiling, eight were boiled in a solution of neutrase enzyme and three were boiled in a mixture of neutrase enzymatic washing powder (Biotex) and a detergent. Six of the nine animals defleshed by simmering were simmered in a Biotex solution, one in a neutrase solution and two in a combination of both neutrase and Biotex. Maceration was used to deflesh 24 of the animals. Of these, 17 were macerated in neutrase solutions while the remainder used one of a combination of neutrase, Biotex and detergent solutions. 14 of the 20 skeletons that were prepared by burial were simply buried in leaf mould. The remaining six animals were either buried in other soil types or buried and then either boiled or macerated. The method used to deflesh 31 of the animals was not known. The details regarding the method used to deflesh any particular animal are available in appendix B. However, no details as to the exact nature of the soil, strength of solution, temperature or duration of treatment were available. The preparation methods used are broadly described by Davis and Payne (1992).

### 7.2.4: Age

The dates of birth and dates of death of the individuals analyzed in this project were known. These were used to calculate the age (in days) of the animals. Occasionally the exact date of birth or death was not known and so the age in days was approximated. Even in these cases, the margin of error was never greater that 30 days and was usually less than 15 days. Such small potential differences in age are unlikely to have any measurable impact on the bone density of the material and so are acceptable. The sole exception to this was animal number 1307, which had a margin of error of +/- 45 days. Given that this animal was 4324 days old, this margin of error was also deemed acceptable.

Three of the animals died before birth. These animals are two very immature twins and a single slightly more developed individual. The ages at death of these animals are unknown. However, the twins are about eight times smaller than the more developed animal and so are likely to be considerably younger than the single larger individual. The twins have been defined as "fetal" while the larger animal is described as "stillborn" (see table 7.5). This terminology is simply intended to express a difference in age of these animals and does not refer to any strict developmental definitions.

The actual ages of all of the individuals from the experimental material are displayed in tables 7.4, 7.5 and 7.6 (see section 7.2.6).

### 7.2.5: Month of death

Since the month in which an animal died can affect the density of its skeleton (especially in pregnant or lactating females - see section 5.2.6), this information was noted for each of the animals used in this project. Table 7.3 shows the frequency of animals that died or were killed in each month.

| Month of Death | January | February | March | April | May | June | July | August | September | October | November | December |
|---|---|---|---|---|---|---|---|---|---|---|---|---|
| Number of individuals analyzed | 8 | 10 | 8 | 9 | 2 | 2 | 5 | 5 | 12 | 6 | 10 | 18 |

***Table 7.3: Showing the number of animals in the experimental material that died in each month of the year.***

### 7.2.6: Material distribution and analytical method

In order to assess the potential impact of any one of the specified variables on the density of an animal's skeleton it will be necessary to examine pairs or groups of animals that differ by only one attribute. By doing so, any variation in bone density between individuals in these groups can be assumed to be the result of the unmatched variable. It is for this reason that further description of the attributes of the experimental material is required. Tables 7.4, 7.5 and 7.6 display the attributes of all of the animals used in this project. Where more than one individual with the same attributes was used, the ages of all such animals are shown. These tables also display the ages of the animals examined in this project.

| Sex | Preparation Method | Month of Death | Age in Days | | | | | | | | |
|---|---|---|---|---|---|---|---|---|---|---|---|
| Male | Boiling | November | 950 | | | | | | | | |
| Male | Boiling | December | 950 | 954 | 960 | | | | | | |
| Male | Simmering | March | 331 | 694 | | | | | | | |
| Male | Maceration | February | 668 | | | | | | | | |
| Male | Unknown | September | 863 | 864 | | | | | | | |
| Male | Unknown | February | 657 | | | | | | | | |
| Female | Maceration | December | 1691 | 1691 | 1691 | 2056 | 2056 | 2421 | 2421 | 2421 | 2421 |
| Female | Unknown | January | 2473 | | | | | | | | |
| Female | Unknown | December | 1691 | | | | | | | | |
| Castrate | Boiling | October | 556 | | | | | | | | |
| Castrate | Boiling | November | 950 | 954 | 1309 | | | | | | |
| Castrate | Simmering | March | 693 | | | | | | | | |
| Castrate | Simmering | April | 1094 | | | | | | | | |
| Castrate | Maceration | January | 607 | | | | | | | | |
| Castrate | Maceration | April | 340 | 704 | | | | | | | |
| Castrate | Maceration | June | 442 | | | | | | | | |
| Castrate | Maceration | July | 801 | 1186 | | | | | | | |
| Castrate | Maceration | December | 238 | 970 | | | | | | | |
| Castrate | Unknown | January | 610 | 1371 | 1375 | | | | | | |
| Castrate | Unknown | April | 707 | 1076 | | | | | | | |
| Castrate | Unknown | May | 1116 | | | | | | | | |
| Castrate | Unknown | July | 447 | 813 | 1198 | | | | | | |
| Castrate | Unknown | September | 1600 | 1600 | | | | | | | |
| Castrate | Unknown | October | 563 | | | | | | | | |
| Castrate | Unknown | November | 920 | 951 | 1291 | | | | | | |
| Castrate | Unknown | December | 230 | | | | | | | | |

***Table 7.4: Showing the attributes for the Shetland sheep from within the experimental material.***

| Sex | Preparation Method | Month of Death | Age in Days | | | | | |
|---|---|---|---|---|---|---|---|---|
| Female | Boiling | August | 2703 | | | | | |
| Female | Simmering | November | 2765 | | | | | |
| Female | Maceration | January | 3839 | 3944 | | | | |
| Female | Maceration | April | 3670 | | | | | |
| Female | Burial | February | 3607 | | | | | |
| Female | Burial | June | 3345 | | | | | |
| Female | Burial | September | 1258 | 1259 | 1277 | 2711 | 3794 | 4175 |
| Female | Burial | October | 4950 | | | | | |
| Female | Unknown | January | 1381 | | | | | |
| Female | Unknown | February | 305 | 649 | 3961 | 4324 | | |
| Female | Unknown | August | 3368 | | | | | |
| Female | Unknown | September | 1642 | | | | | |
| Castrate | Maceration | May | 4791 | | | | | |
| Castrate | Maceration | October | 579 | | | | | |
| Castrate | Maceration | December | 954 | | | | | |

***Table 7.5: Showing the attributes for the Soay sheep from within the experimental material.***

| Sex | Preparation Method | Month of Death | Age in Days | | |
|---|---|---|---|---|---|
| Male | Simmering | March | 1430 | | |
| Male | Burial | April | 3 | 4380 | |
| Male | Burial | August | 161 | 171 | 182 |
| Male | Burial | September | 518 | | |
| Female | Simmering | March | 335 | 3285 | |
| Female | Simmering | November | 1322 | | |
| Female | Burial | February | Fetal | Fetal | 3252 |
| Female | Burial | March | 3992 | | |
| Female | Burial | November | 1322 | | |
| Female | Unknown | April | Stillborn | | |
| Castrate | Boiling | October | 531 | 541 | |

***Table 7.6: Showing the attributes for the sheep of "other" breeds from within the experimental material.***

It should be noted from tables 7.4, 7.5 and 7.6 that the material is not evenly distributed. For example, none of the animals analysed were male Soay sheep. Examining groups of animals of similar, rather than identical, ages or month of death will enable more matched pairs to be located. This is only possible if it can be assumed that animals that differ by only one or two months in age (or months of death) are effectively the same in terms of bone density. The gaps within the experimental material will mean that producing statistically robust inferences from the density data is impossible. Instead only broad pattern and suggestions will be able to be made. The

problems caused by the unequal distribution of the experimental material will be returned to in chapter 8. The implications of or alternatives to examining a fully representative experimental sample are discussed in section 10.3.1.

## 7.3: Methods

Section 6.4.6 outlines the criteria that must be considered when designing a method for measuring the radiodensity of bone. These criteria suggest the use of a method based on photodensitometry, due to the low cost, high accessibility and relatively high levels of precision and accuracy of this method. This method will be described in detail below, but first it would be appropriate briefly to mention two important requirements of the method.

Photodensitometry relies on the determination of the radiodensity of bone (or other material) through the examination of a radiographic image of a specimen. Radiodense material appears in a radiograph as a comparatively light grey image. Radiolucent material (that with a low radiodensity) appears as a darker grey image. The radiodensity of a bone specimen can be described as being the product of a combination of its size and its bone density. An increase in either bone density or bone size will produce a paler image. There are therefore two important requirements of the method that will be used in this project. First, it must be able to quantify objectively how light or dark grey each image (or part of each image) is. Secondly, it must enable the size of each bone to be measured and accounted for, so that differences in the grey level of the radiographic images can be attributed to variations in bone density alone. These and other considerations will be addressed below.

The need to ascertain the size of a bone specimen has presented considerable problems for photodensitometry and many other methods mentioned in section 6.2. The need to establish the size of a specimen has often resulted in attempts to measure the cross-sectional dimensions of the sample being measured. These attempts can rarely be assumed to be either accurate or reliable. In clinical studies this does not present a problem, since such studies are most often longitudinal or compare only one element at a time. This means that the cross-section remains roughly constant. Unfortunately, this is not the case for the material to be used in this project. QCT (quantitative computed tomography – see section 6.3.6) ascertains the cross-section of the material under investigation by taking multiple measurements of the sample at different orientations. A

slightly cruder method of replicating this effect in photodensitometry is to make two radiographs of each element to be measured: one at 90° to the other. This produces a paired set of radiographs, the first of which can be used for making photodensitometry measurements, while the second will provide a cross-section of each bone, from which the bone thickness can be read. This is the procedure that will be followed in this project.

For each bone that was to be measured, two radiographs were therefore needed. The first (referred to here as the *density* or "D" radiograph) was to provide an image from which a radiodensity measurement could be taken. The second was taken after the bone had been rotated by 90° about its long axis. This second image (the *thickness* or "T" radiograph) provided a "side view" of each bone and enabled the thickness of the bone at each scan-site to be measured, so that the effects of bone thickness on radiodensity can be accounted for. A 90° rotation was obtained for each bone by mounting it on a right-angled bracket. Figure 7.2 shows how the use of the bracket enabled an accurate and repeatable rotation between each paired set of radiographs.

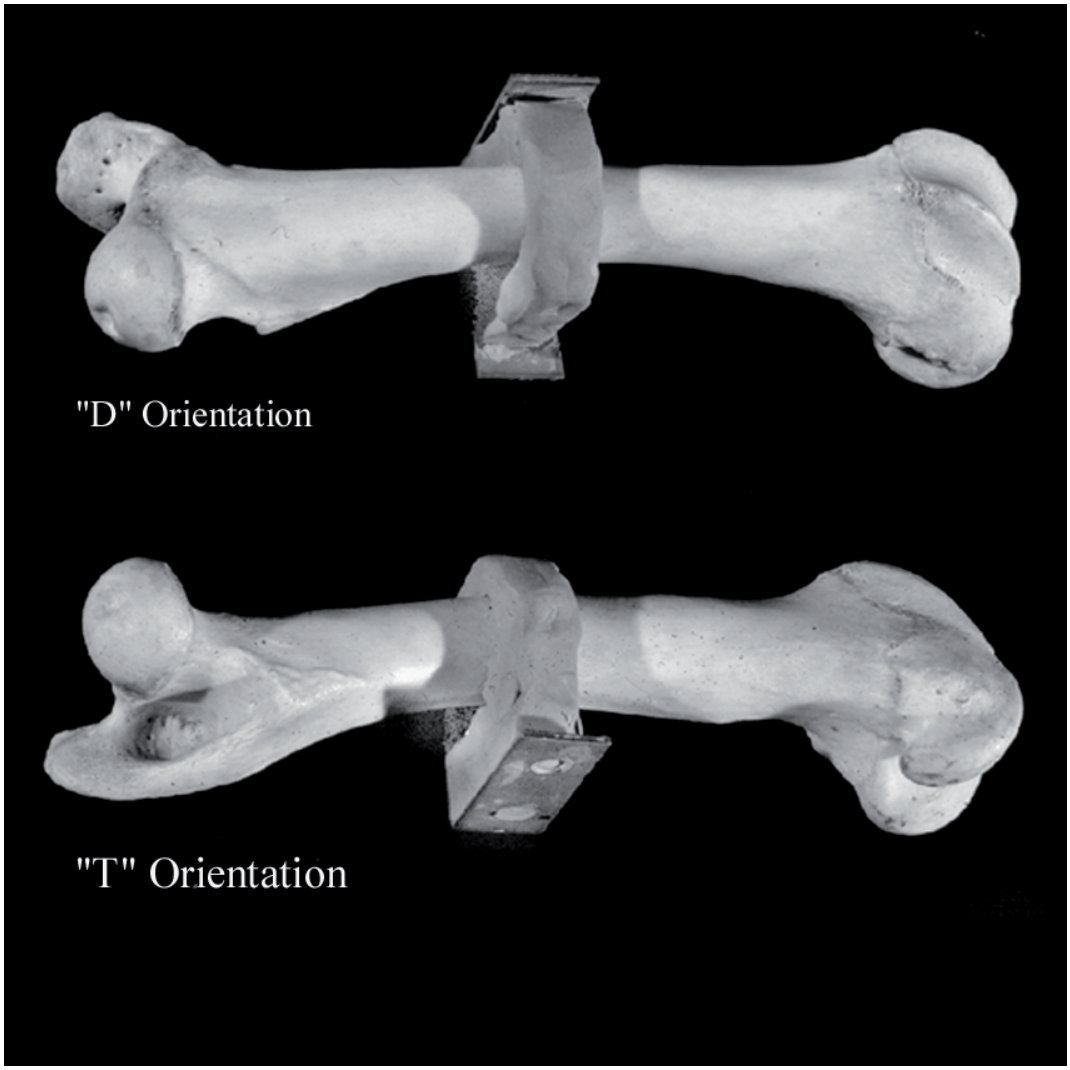


***Figure 7.2: Showing two views of a femur mounted on a right-angled bracket. This bracket enables the bone to be rotated by 90° so that the "D" and "T" orientations can be obtained.***

The scan-sites were marked on each bone by attaching a small arrow of self-adhesive lead to the bone before it was radiographed. Since lead is very radiodense, these markers were apparent on the images as white arrows indicating each scan-site. The lead markers enabled scan-sites to be standardised, with reference to the external morphology of each bone, since external morphological features were not visible on the radiographic images. Furthermore, provided that the markers were not repositioned between radiographic exposures, the identical point was marked on both the "D" and the "T" radiographs. This ensured that the bone thickness was measured at exactly the same position as the radiodensity (see figure 7.4).

The criteria for choice of scan-sites are laid out in section 6.4.4. A detailed description of the position of each scan-site is given below. Note that each scan-site takes the form of an approximately 0.05 $cm^2$ area of bone. This is in contrast to the linear measurements used by Butler and Chatters (1994), Elkin (1995), Kreutzer (1992), Lyman (1984) and Willey *et al* (1997). By using linear scan-sites, these researchers had to overcome the problem of measuring the thickness of the bone, in order to transform their linear density measurements into volume density measurements. In doing so they often had to resort to either the (incorrect) assumption that the bones had a regular cross-section (see section 6.2.5), or some approximation of the bone's cross-section (Kreutzer 1992 p284). Selecting what is effectively an individual point for each scan-site will overcome this problem, because, provided that the bone thickness is measured at the same point as the scan-site, the bone thickness used will be an accurate representation of the thickness of the bone *at the point of measurement*.

### 7.3.1: Location of scan-sites

The choice of scan-site locations has already been discussed (see sections 6.4.4 and 7.1.3). The position of the scan-sites are shown in figure 7.1. The scan-sites are described and shown in more detail in appendix A.

### 7.3.2: Taking the density measurements

To ensure that the results produced were consistent, the procedures described below were followed. Any slight deviations in these procedures (eg variations in the chemical strength when developing the radiographs) were rectified by calibrating the radiographic images, using the method described below.

All radiographs were taken on Kodak Industrex AA400 "ReadyPack" 18x24 cm film using a custom built Todd Research X-ray cabinet. The source - film distance was 556 mm and a 0.2 mm aluminium filter was used. The material was exposed at 50 KV and 3 ma. Exposure time was either 25, 35, 70, or 80 seconds, depending on the age and size of the animal being examined (with young or small individuals being exposed for less time than older or larger animals). All bones were exposed along with a step wedge composed of aluminium and consisting of 15 steps, ranging from 1 mm to15 mm in thickness of equal (1 mm) graduations.

The radiographs were developed in deep tanks under red safe light at 20°C. Each radiograph was developed in Kodak HC110 developer, diluted with water (1:31) for 9 minutes (developing time was gradually increased to 15 minutes as the developer aged).

Whilst developing, the films were agitated every three minutes. Once the development had been stopped (by immersion in “stop solution” for 10-20 seconds) they were fixed for 5 minutes and washed for 15 minutes.

The developed radiographs were converted into digital images by means of a desktop scanner. They were scanned on an *AGFA Duoscan T1200* desktop scanner (which incorporates an attachment for scanning large transparencies). The images were scanned at 100%, as 300dpi greyscale TIFF (tagged image file format) images.

Radiodensity measurements were made using specially designed image analysis software. The software in question was the *Scion Image* package and is available on the Internet at www.scion.com. Each pixel of all greyscale TIFF images is assigned a value of between 0 and 255 that relates to the greyscale of that particular pixel (where 0 is white and 255 is black). The greyscale of any part of a radiograph relates to its radiodensity: a low greyscale (light) indicating a high radiodensity, while a high greyscale (dark) indicates a low radiodensity. Therefore, by calculating the average greyscale of a specified part of an image, Scion Image is able to provide an indication of the radiodensity of any part of the scanned radiographs.

Each image was standardised at this stage by measuring the greyscales of each step of the step wedge. This produced 15 measurements per radiograph, each of which could be assigned a “known density” (the thickness of aluminium). The computer package was able to interpolate between and extrapolate from these 15 greyscales of “known density” so that all 255 greyscales could be assigned an equivalent thickness of aluminium (see figure 7.3).

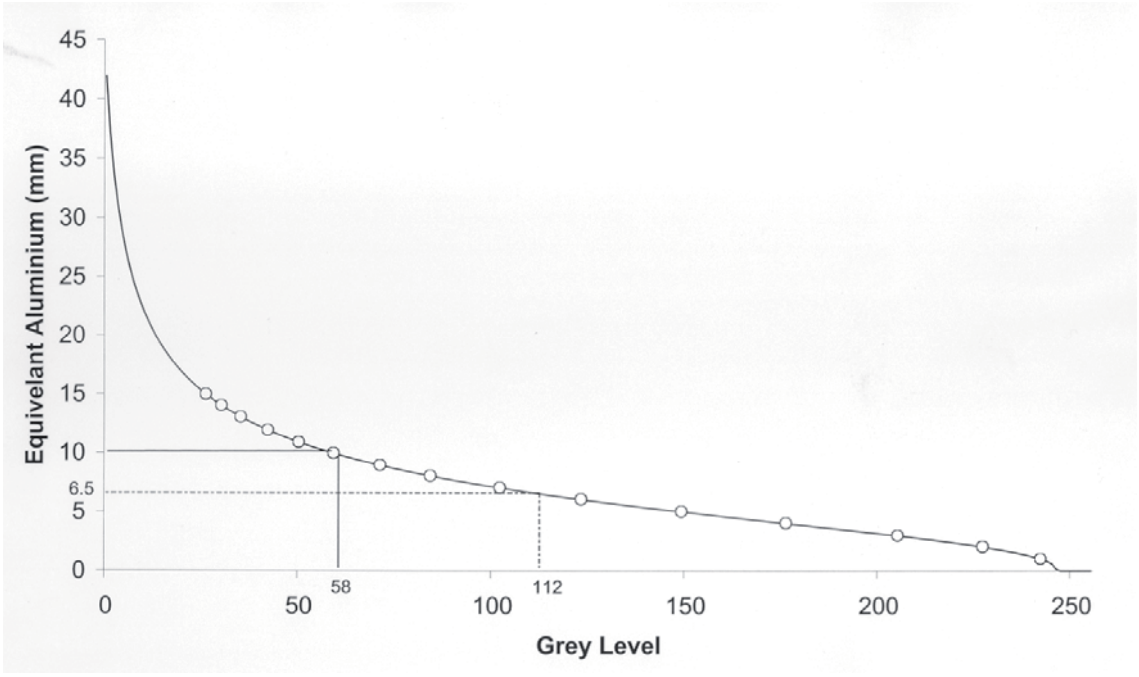


***Figure 7.3: Showing a calibration curve, as produced by this project. The grey scales produced by a known thickness of aluminium are shown as white circles, eg 10 mm of aluminium appears on the scanned radiograph as a greyscale of 58. All 15 greyscales associated with a known thickness of aluminium are combined to produce a curve from which every greyscale can be attributed an equivalent thickness of aluminium. This curve can be used to establish, for example, that a greyscale of 112 is equivalent to 6.5 mm of aluminium.***

This process had the effect of overcoming any variations in the exposure or developing of the radiographs. It also resulted in the measurements effectively being in millimetres (indicating the thickness of aluminium that would have the same radiodensity as any particular scan-site).

Each measurement was taken by highlighting an approximately 0.05 $cm^2$ area of the radiograph at the position of the scan-site, using the selection tool available in Scion Image, and selecting "measure" from the "analysis" menu. The values returned were the averages of the selected pixels and could be exported directly to a database.

### 7.3.3: Measuring bone thickness

A perceived problem faced by many previous researchers was that it was impossible to overcome the effects of any air-filled medullary cavity within the bone (eg the marrow cavity that occupies the core of long bone shafts). Previous researchers have suggested that their results would be improved significantly if they could account for these air spaces. They reasoned that, since such spaces have an effective density of

zero, including them in their calculations would have the effect of greatly reducing the density value finally produced. By incorporating the air-filled medullary spaces into their calculations, these researchers have effectively been producing density values that represent an *average* for the whole bone thickness, *including the air space*. Lam *et al* (1999) used QCT to remove the effects of the medullary spaces on their calculations. In doing so, they produced values that related to the bone material itself. Unsurprisingly, the results produced by Lam *et al* were up to 40% higher than those returned by Lyman (1984).

It is therefore necessary to decide which of these two methodologies would be most appropriate for this project. Should the data reflect the properties of only the cortical bone, or an average of the entire bone cross section? Later, this project will be investigating the destruction of *whole* bones. It will therefore be more concerned with the strength of complete bones (including medullary and other air spaces) rather than of the bone material itself. Measuring the entire bone thickness (including medullary spaces) will provide data that are relevant to the bone as a whole (or at least in the region of the scan-site in question). It is for this reason that this project will use the thickness of the whole bone to determine its density. In doing so, a thin walled bone shaft would be defined as being less dense than a thick walled bone shaft, even if the density of the bone material itself was identical in each case. Such a calculation is appropriate, because the thin walled specimen would be expected to be less durable in the archaeological record.

The bone thickness was measured as follows. A line was marked on the “T” radiograph, passing through each scan-site and running parallel to the edge of the bracket on which the bone was mounted. This represented the path taken by the X-rays as they passed through each scan-site (figure 7.4).

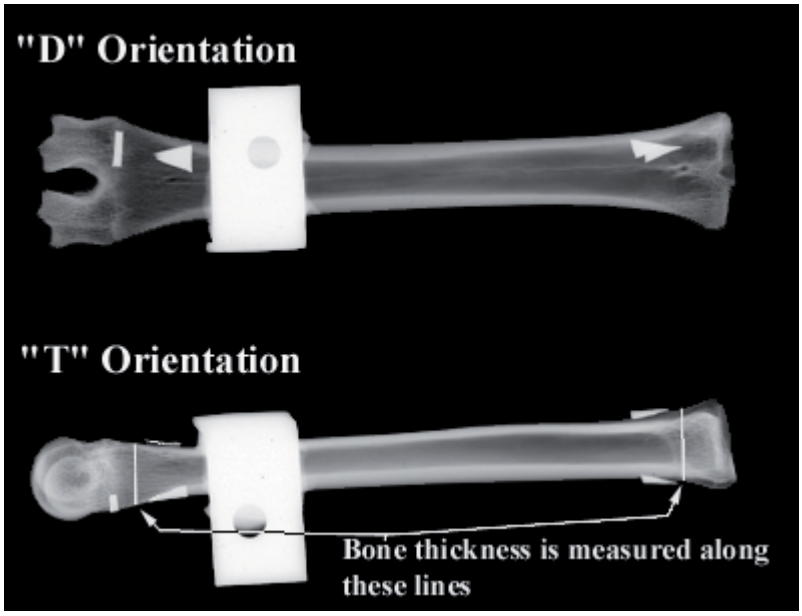


***Figure 7.4: Showing radiographs of a metacarpal in the "T" and the "D" orientations. The scan-site on both orientations is marked. It is possible to use the "T" orientation to establish the thickness of the bone at the scan-site.***

The total thickness of bone and air through which the line passed was measured to the nearest 0.01 cm using dial callipers and entered onto the database.

At this stage, sufficient data were theoretically available to calculate the radiodensity of each scan-site. By dividing the thickness of the bone at each scan-site by the density value returned by Scion Image, a value for the bone density of each scan-site should be returned. However, before this calculation can correctly be executed, it is necessary to ensure that the method is producing accurate and reliable results.

It is certainly worth noting at this point that this methodology is neither intended nor expected to produce data that describe any single physical property of the experimental material. Instead the data will represent some hybrid of bulk density, mineral content and morphology of the bone. It is intended that the data produced here reflect the durability of bone under destructive taphonomic conditions. The extent to which this is the case will be assessed in subsequent sections of this project.

### 7.3.4: Summary (materials)

For this project, sheep has been selected as the most suitable taxon for investigation. The scapula, humerus, radius, metacarpal, pelvis, femur, tibia, metatarsal and first phalanx have been selected as the most suitable elements for measurement. Scan-sites are to be located on the proximal and distal ends and mid-shaft regions of the long bones and, where possible, are to coincide with Watson's "diagnostic zones" (Watson 1972). The sheep skeletons required are to be borrowed from English Heritage's Ancient Monuments Laboratory, in Portsmouth. The material comprises 95 modern sheep skeletons with a range of (known) ages at death, months of death, sexes, breeds and methods of preparation. By comparing groups of animals that differ by only one variable it will be possible to assign any differences in density to variation in that attribute.

### 7.3.5: Summary (methods)

The methods to be used in this project will be applied to a range of scan-sites on elements that have been specifically selected to produce the most applicable and reliable results possible. Bone density, as defined by this project, will be calculated by dividing the radiodensity of each scan-site by the thickness of the bone at that point. Radiodensity will be measured digitally from a radiograph, while bone thickness will be measured from a similar, orthogonal, radiograph.

The data produced are not intended to represent any single physical property of bone, although they are expected to relate to the ability of material to withstand taphonomic destruction.

## 7.4: Methodological Tests

In order to ensure that the methodology described in the previous section would produce reliable and meaningful results that were influenced only by known variables, a series of methodological tests was necessary. Below are descriptions of a number of tests that were carried out in order to assess the reliability of the methods.

### 7.4.1: The representativeness of the results

In order to ensure that the results obtained by this project were an accurate reflection of "true density" it was necessary to compare density measurements derived

by the method proposed in this project with the known density of a set of specimens. Naturally, any method used to calculate "true density" must produce results that are as accurate as possible. A variation on the "direct density measurements" discussed in section 6.3.8 was used here, because it involves calculating only the mass and volume of a specimen in order to determine its density. Since this methodological test intended only to compare radiographically derived densities with directly measured densities, the taxa, age, sex and breed of the material used and the scan-sites chosen were of little consequence.

A selection of material (largely from sheep of indeterminate age, sex and breed, but including two sections through a pair of archaeological human lumbar vertebral bodies) was measured using the procedures outlined for this project (see section 7.3). The scanned areas were marked on each element. A 5 mm thick section was then removed from this material at each scanned point and weighed. Both of the cut surfaces of each of these sections were then photographed with a 20.00 mm scale. The photographs were then digitised to a resolution of 0.2 mm, using a "Calcomp drawingboard III" digitising tablet, and the cross-sectional area of each cut surface was calculated using a geographical information system (GIS) software package ("ArcView"). The average area of the two cut surfaces multiplied by the thickness of each slice provided an indication of their volumes. By dividing the mass of each slice by its volume, a figure for its "true density" was obtained. This measurement is a close approximation of "bulk density" since it does not take into account variations in the mineral content of the bones, beyond what is apparent though variations in their weights. This method of calculating true density is similar to that used by Brickley (1997 p142) to produce values for her "base line density" against which she could compare other experimentally derived density data, and will be referred to here as "base line density".

Digitising a photograph of a single specimen ten times and comparing the resulting surface area calculations assessed the repeatability of the digitising stage of this method. The standard deviation of the ten results produced by this process was 0.007, while the coefficient of variation was 0.002 (0.2%). This is comparable to the results obtained for this measurement by Brickley (1997 p143).

The radiographically derived and base line density values are displayed in tables 7.7. The data from which these measurements are derived can be viewed in appendix B

| Measurement Code | Radiographically Derived Density | True Density ($g/cm^3$) |
|---|---|---|
| P1 | 0.233 | 0.567 |
| P3 | 0.162 | 0.786 |
| S3 | 0.292 | 1.081 |
| D3 | 0.173 | 0.590 |
| P4 | 0.305 | 1.141 |
| S4 | 0.405 | 1.566 |
| D4 | 0.207 | 0.789 |
| P5 | 0.287 | 0.677 |
| S5 | 0.265 | 1.002 |
| D5 | 0.140 | 0.579 |
| 6 | 0.230 | 0.509 |
| 7 | 0.129 | 0.306 |
| D14 | 0.201 | 0.904 |
| S14 | 0.332 | 1.390 |
| P16 | 0.334 | 1.004 |
| AC9 | 0.198 | 0.438 |
| IL9 | 0.204 | 0.523 |
| P10 | 0.255 | 0.674 |
| S10 | 0.246 | 0.979 |
| D10 | 0.143 | 0.615 |
| S12 | 0.389 | 1.190 |
| D15 | 0.325 | 0.846 |
| P15 | 0.213 | 0.939 |
| S15 | 0.364 | 1.426 |
| S13 | 0.555 | 1.605 |
| P13 | 0.309 | 0.914 |

***Table 7.7: Showing the radiographically derived density values (using the methodology proposed for this project) and the base line density values for a set of elements. The radiographically derived density values have been corrected for the effects of magnification. For an explanation of this, see below.***

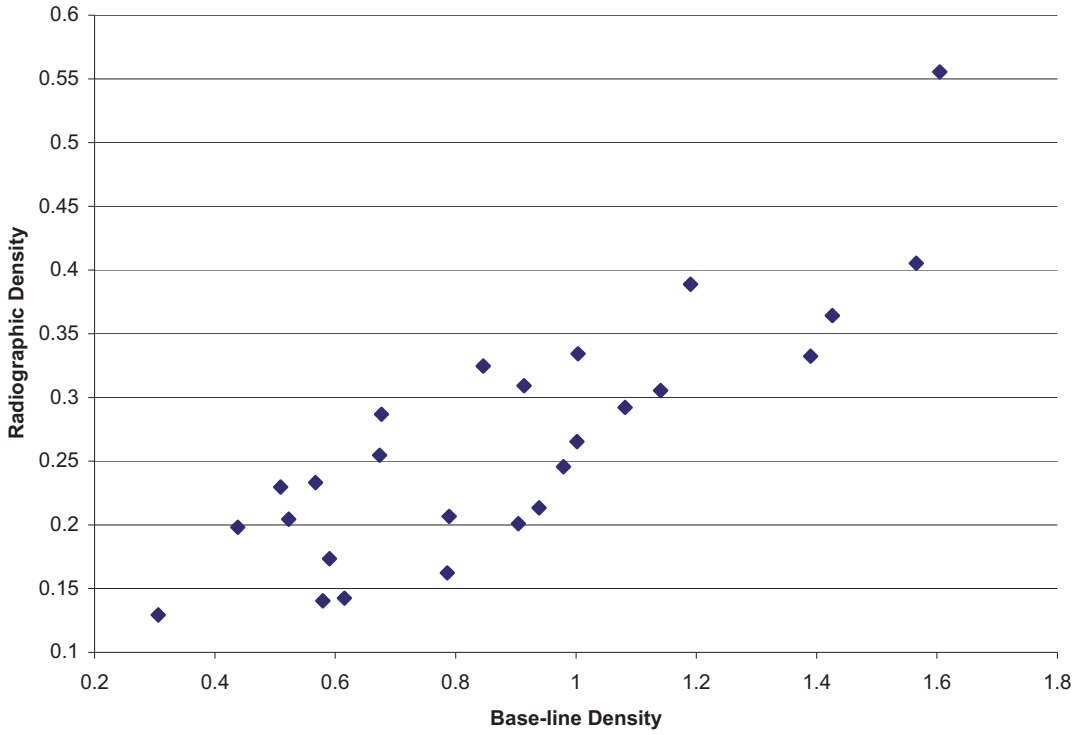


***Figure 7.5: A scatter-plot of radiographically derived density against base line density, showing an increase in base line density being matched by an increase in radiographically derived density.***

By plotting the two measures of density against each other, it is possible to assess how radiographically derived density relates to base line density (see figure 7.5).

The points on figure 7.5 show a strong positive relationship between the radiographically derived density of the type employed in this project and base line density. This graph clearly shows a linear relationship between the data produced by the two measurement methods. The linearity of the relationship suggests that the most appropriate statistical method with which to compare them is the Pearson's product-moment correlation coefficient. The two sets of data return a Pearson's product-moment correlation coefficient of 0.842 (significant to the 0.01 level). Consequently, it is possible to conclude that where the method used in this project identifies bones as being of low density, their base line density will be similarly low. This is equally true for higher density readings.

By employing an accurate (but destructive) means of measuring bone density on a small number of bones, and comparing these results with those obtained by

radiographic means on the same material, it has been possible to confirm that radiographically derived density relates closely to base line density.

### 7.4.2: Repeatability of the method: intra-observer error

When taking large numbers of measurements, it is not unlikely that the reliability of the method will be partly dependent on the consistency with which the operator is working. A variety of conscious and subconscious factors can affect this consistency (eg the time of day, lighting conditions, speed at which the operator is working). In order to assess the potential impact of any inconsistency in working method on the results produced, a repeatability or *intra-observer* error test was carried out. This test involved taking four sets of measurements (including re-mounting and radiographing the material) from the same individual and examining any variation between each set. Animal number 59 (a 657 day old male Shetland) was arbitrarily selected for this procedure. The four sets of measurements were taken on different arbitrarily determined days and times of day. The time that elapsed between taking each measurement set varied and is outlined below.

| Measurement Set | Day and Time Taken |
|---|---|
| A | Day 1 (am) |
| B | Day 1 (pm) |
| C | Day 3 (pm) |
| D | Day 6 (am) |

***Table 7.8: Showing the day and time that each measurement set was taken. The days are arbitrarily named (1-6).***

It can be seen from table 7.8 that the time lapse between taking sets A and B is shorter than for B and D. The period between the taking of measurement sets A and D is greater still. The results of this test are shown in table 7.9.

| | Density Measurement Set A | Density Measurement Set B | Density Measurement Set C | Density Measurement Set D |
|---|---|---|---|---|
| **Scap** | 0.302 | 0.300 | 0.303 | 0.310 |
| **P Hum** | 0.198 | 0.197 | 0.189 | 0.187 |
| **S Hum** | 0.302 | 0.311 | 0.301 | 0.301 |
| **D Hum** | 0.344 | 0.346 | 0.341 | 0.350 |
| **P Rad** | 0.294 | 0.303 | 0.294 | 0.297 |
| **S Rad** | 0.408 | 0.423 | 0.415 | 0.421 |
| **D Rad** | 0.322 | 0.333 | 0.325 | 0.315 |
| **P MetaC** | 0.223 | 0.216 | 0.210 | 0.219 |
| **S MetaC** | 0.357 | 0.356 | 0.366 | 0.363 |
| **D MetaC** | 0.182 | 0.187 | 0.175 | 0.181 |
| **P MetaT** | 0.254 | 0.251 | 0.246 | 0.246 |
| **S MetaT** | 0.353 | 0.360 | 0.356 | 0.377 |
| **D MetaT** | 0.283 | 0.282 | 0.277 | 0.274 |
| **P Tib** | 0.166 | 0.157 | 0.153 | 0.154 |
| **S Tib** | 0.445 | 0.450 | 0.453 | 0.443 |
| **D Tib** | 0.203 | 0.197 | 0.200 | 0.211 |
| **Phal1 (7)** | 0.469 | 0.472 | 0.463 | 0.479 |
| **Phal1 (8)** | 0.388 | 0.385 | 0.386 | 0.398 |
| **Phal1 (9)** | 0.412 | 0.398 | 0.409 | 0.412 |
| **Phal1(10)** | 0.421 | 0.412 | 0.422 | 0.429 |
| **P Fem** | 0.257 | 0.255 | 0.260 | 0.261 |
| **S Fem** | 0.189 | 0.201 | 0.184 | 0.188 |
| **D Fem** | 0.189 | 0.178 | 0.190 | 0.186 |
| **Pelv** | 0.334 | 0.332 | 0.320 | 0.333 |

***Table 7.9: Showing the density values produced from the same skeleton on four different occasions. The first phalanx appears four times because a separate measurement was taken for each of the four first phalanges from this specimen.***

The graphical method used to display these data is that proposed by Altman and Bland (1983 pp311 - 314). In their paper, these authors suggested that the correlation coefficient between two repeated sets of measurements was a poor indicator of the repeatability of the measurement method being used (Altman and Bland 1983 pp308 - 310). Instead, they proposed a graphical method that enables sets of measurements to be compared and an assessment made as to whether the magnitude of the true result or the time lapse between measurements impacted on the method's repeatability. The proposed method involved the comparison of two sets of measurements at a time. Each measurement from one set is subtracted from the equivalent measurements from another set and the resulting difference is plotted against the average of the two figures. The intention of Altman and Bland's method was to enable the comparison of the variability of the density measurement method (signified by the density difference) with the true

density value. Since the true density was not actually known, Altman and Bland took the average of the two measurement sets as being its closest possible approximation.

If the two sets of measurements agree exactly, then the points on the graph will form a straight horizontal line. Bland and Altman (1986 p308) suggested that if all of the points on the graph fall within 2 standard deviations of the mean of all of the differences combined, then the method could be described as being reliably repeatable.

Figures 7.6 - 7.11 (overleaf) are the “Bland and Altman” plots for the repeatability test carried out by this project. They refer to comparisons of measurement sets A & B, A & C, A & D, B & C, B & D and C & D.